Modelling and Experiments of a Standing Wave Piezomotor

Andersen, B.; Helbo, Jan; Blanke, Mogens

Published in:
Proceedings of the 8th International Conference on New Actuators

Publication date:
2002

Document Version
Publisher's PDF, also known as Version of record

MODELLING AND EXPERIMENTS OF A STANDING WAVE PIEZOMOTOR

B. Andersen, J. Helbo
Department of Control Engineering, Aalborg University, Aalborg, Denmark.

M. Blanke
Department of Automation, Technical University of Denmark, Kgs. Lyngby, Denmark.

Abstract:
The paper presents a new contact model for standing wave piezomotors. The contact model is based on the Hertz theory for normal contact deformations and elastic contact theory for tangential loads. The contact theory is simplified into a model with discrete springs for normal and tangential loads which allows the calculation of slip/stick transitions. Simulations show that tip trajectories in general cannot be prescribed. The paper presents the principle of a bending resonator. Experiments indicate that the bending vibrations are too small to generate rotor rotations. However, due to unintended excitation of other modes motor performance was achieved.

Introduction

One type of standing wave piezomotors is based excitation of two mutually independent vibration modes e.g. a longitudinal mode and a torsion mode. This paper presents a resonator that generates contact trajectories from excitation of bending vibrations only. It is possible to excite the resonator in two ways; either it is excited to generate a trajectory that has the shape of a number 8 or it is excited to generate an elliptic trajectory.
Many researchers have analysed contact models for travelling wave motors. However, there are few examples for the intermittent contact type motor that includes the elastic contact properties. The contact effects of standing wave motor was analysed in [4] by using a finite element model. In this analysis the motion of the contact tip and rotor velocity is prescribed. Therefore, this analysis does not describe how the dynamics of the contact tip and rotor is affected by the contact.
In [7] the contact of a piezomotor was analysed analytically by using Hertzian contact theory and elastic tangential contact theory. Again this analysis assumes a prescribed tip trajectory and it does not deal with calculation of the rotor dynamics.
This paper presents a contact model for a standing wave piezomotor based on the elastic properties of the contact zone. From the general contact model a simplified discrete spring model is derived. The model presented here does not assume a prescribed tip trajectory or a prescribed rotor velocity. The resonator is modelled based on Hamilton's equations. The principle and design of the piezomotor are explained. Simulation results based on the resonator design are presented as well as experimental results.

Resonator design

The resonator is designed as a simple supported beam. In practice the support of the beam is realised with a thin strip of material connecting the beam to the remaining construction. The thickness of the strip is 0.2 mm. The resonator construction is placed on plate springs for generation of a preload. The design was motivated by the paper [6] and through discussions with the author of that paper.
In order to generate elliptical trajectories the resonator is excited with the voltage signal

$$U_A = U_0 \sin(2\pi f) \text{ and } U_B = U_0 \sin(2\pi f + \pi/2) \quad (1)$$

where U_0 is the voltage amplitude. For generation of 8-number shaped trajectories the excitation signal is

$$\begin{aligned} U_A &= U_1 \sin(2\pi f_1) + U_2 \sin(2\pi f_2) \\ U_B &= U_1 \sin(2\pi f_1) - U_2 \sin(2\pi f_2) \end{aligned} \quad (2)$$

where U_1 and U_2 are voltage amplitudes and the ratio f_2/f_1 must equal 2.

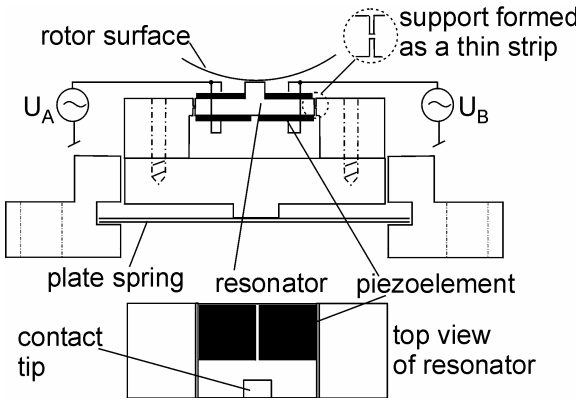

***Fig 1**: Resonator design and voltage excitation.*

Resonator equation

The derivation of the resonator model takes a starting point in Hamilton's principle for an electromechanical system [2].

$$\int_{t_1}^{t_2} \left[\delta(T - U + W_e) + \delta W\right] dt$$

where δ is the variational operator, T is kinetic energy, U is strain energy, W_e is electric energy and W represents energy from applied external point forces. The energy expressions are derived by using the Rayleigh-Ritz approximation with mode shapes for a simple supported Bernoulli-Euler beam. The detailed derivations are given in [1]. The result is the resonator equation which is given by

$$\mathbf{M}\ddot{\mathbf{r}} + \mathbf{C}\dot{\mathbf{r}} + \mathbf{K}\mathbf{r} = \mathbf{Q}_F + \mathbf{Q}_T \qquad (3)$$

where **M, C** and **K** are matrices for mass, damping and stiffness, $\mathbf{Q}_F$ and $\mathbf{Q}_T$ represents applied generalized force and torque and **r** is the vector of generalised coordinates. The damping is given by $\mathbf{C} = \alpha\mathbf{M} + \beta\mathbf{K}$ with $\alpha = 1.2 \cdot 10^3, \beta = 4.1 \cdot 10^{-8}$.

Contact model

The contact model is derived from the Hertzian contact theory and from theory for the elastic tangential deformations and tractions. However, since not all information given by the general theory is needed for the calculation of the contact forces a simplified model is derived.

For the modelling the following assumptions have been taken: Perfect elastic behaviour, independence of normal pressure and tangential tractions and the quasi-static approach [3]. In order to use the general theory the contacting bodies are described as spherical surfaces although the rotor is of course not cylindrical. Finally, the rotation of the rotor is neglected so the motion is described as purely rectilinear. The Hertz theory gives the relation between normal force and contact deformation as follows [3]

$$F_N = K_N \delta^{3/2} \quad \text{with} \quad K_N = \tfrac{4}{3}\sqrt{R^*}E^* \qquad (4)$$

with stiffness $E^* = \frac{1-\nu_1^2}{E_1} + \frac{1-\nu_2^2}{E_2}$ and relative radius $R^* = (R_1^{-1} + R_2^{-1})^{-1}$. The relation between the normal force and the distribution of normal pressure as well as the relation between contact radius and normal force is given by

$$F_N = \int_0^a p(r) r\, dr = \tfrac{2}{3} p_0 \pi a^2 \quad \text{and} \quad a = \left(\frac{3F_N R^*}{4E^*}\right)^{1/3} \qquad (5)$$

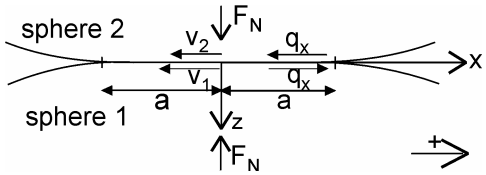

***Fig 2**: Sliding contact of two spheres.*

where r is the radial coordinate of the contact circle. A situation with two sliding spheres is show in figure 2. The velocities v_1 and v_2 are the tangential velocities of the surface points at the origin of the contact circle. Since v_1 and v_2 are different in magnitude the centre points are sliding and, thus, the rest of the contact area will also be sliding [3]. By using Coulomb's friction law the tangential tractions q_{x1}^{sl} and displacements u_{x1}^{sl} are given by [7], [5]

$$q_{x1}^{sl} = \mu p_0 \sqrt{1 - \tfrac{r^2}{a^2}}, \quad 0 \le |r| \le a \qquad (6)$$

$$u_{x1}^{sl} = \mu p_0 \frac{2 - \nu_1}{8 G_1 a}\left(2a^2 - r^2\right)\tfrac{\pi}{2}, \quad 0 \le |r| \le a \qquad (7)$$

and similarly for sphere 2 but with opposite sign. The modulus of elasticity in shear is $G = \frac{E}{2(1-\nu)}$.

When stick initiates the stick zone will start at the centre of the contact circle and then spread outwards, thus, the inner circle is in the state of stick and the outer ring is in the state of slip [3]. The solution for tangential traction and displacement in the stick zone is given by

$$q_{x1}^{st} = -\frac{c}{a} p_0 \sqrt{1 - \tfrac{r^2}{c^2}} + \mu p_0 \sqrt{1 - \tfrac{r^2}{a^2}}, \quad 0 \le |r| \le c \qquad (8)$$

$$u_{x1}^{st} = \frac{\pi \mu p_0}{8 G_1 a}(2 - \nu_1)\left(a^2 - c^2\right), \quad 0 \le |r| \le c \qquad (10)$$

where c is the radius of the stick zone [7], [5]. The corresponding expressions for the outer ring of slip have been omitted. From (10) it is seen that the displacements are constant over the stick zone. The relation between friction force and normal force in the case of stick can be found as follows [3]

$$F_\mu = \int_0^a q_{x1}^{st} r\, dr = F_N \mu \left(1 - \frac{c^3}{a^3}\right) \qquad (12)$$

Since stick is initiated at the centre of the contact circle the time for the slip to stick transition can be found by comparing the surface velocities $v_1 = v_{tip} + \dot{u}_{x1}$ and $v_2 = \Omega R_{rotor} + \dot{u}_{x2}$ at $r = 0$.

Because of this, and since forces are required but not tractions and pressure, the model shown in figure 3 is suggested for the contact model. The springs for tangential stiffness k_{t1} and k_{t2} are nonlinear springs with a force-displacement relation that is dependent on contact forces and whether the contact is in the state of slip or stick.

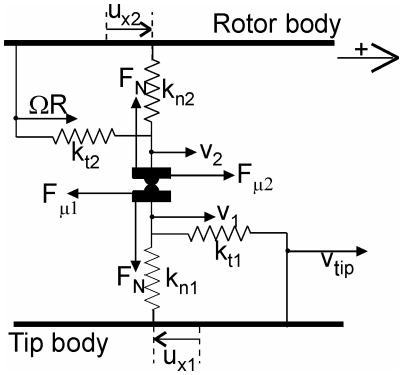

***Fig 3**: Simplified contact model.*

By using equations (5) and (7) the relation between friction force and displacement at $r = 0$ is given as

$$u_{x1}^{sl} = -\text{sign}(v_1 - v_2)\mu K_{t1} F_N^{2/3} \tag{13}$$

$$\text{with} \quad K_{t1} = \left(\frac{4E^*}{3R^*}\right)^{1/3} \frac{3(2-\nu_1)}{16G_1} \tag{14}$$

The sign function was introduced to give the correct relation between the relative velocities and the sign of displacement. Equation (13) is used for calculation of u_{x1}^{sl} and $\dot{u}_{x1}^{sl}$. By using equations (5), (10) and (12) the displacement in the stick zone can be formulated as

$$u_{x1}^{st} = -\text{sign}(u_{x1}^{st})\mu K_{t1}\left(F_N^{2/3} - \left(F_N - \frac{F_\mu}{\mu}\right)^{2/3}\right) \tag{15}$$

and similarly for u_{x2}^{st}. When u_{x1}^{st} and F_N are known eq. (15) can be used to determine the friction force.

Implementation of the contact model

In order to derive the deformation δ and thereby the normal force the geometry of the contact tip and rotor shown in figure 4 is used.

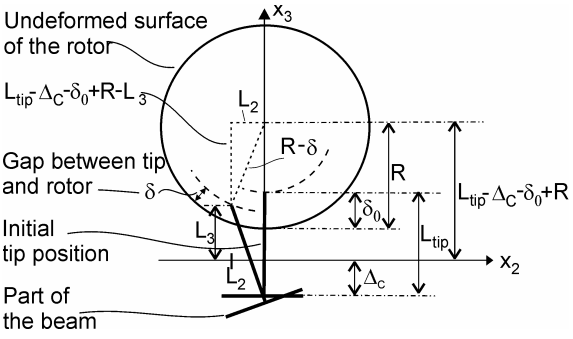

***Fig 4**: Geometry of the contact.*

By moving the elasticity of the surface of the tip to the surface of the rotor the deformation is estimated with a number of uccessive calculations of δ. From figure 4 the constraint equation for the tip trajectory is given as

$$(R-\delta)^2 = L_2^2 + \left(L_{tip} - \Delta_C - \delta_0 + R - L_3\right)^2 \tag{16}$$

from which δ can be calculated when the position of the tip (L_2,L_3), the initial deformation δ_0 and the initial bending of the beam Δ_C are known. During stick the total deformation $u_{x1}^{st} - u_{x2}^{st}$ only depends on the tip and rotor velocity. Thus, the total deformation can be estimated as follows

$$u_{tot}(t_{n+1}) = u_{tot}(t_n) + \Delta t\left(v_{tip}(t_n) - v_{rotor}(t_n)\right) \tag{17}$$

Equation (15) gives the ratio between u_{x1}^{st} and u_{x2}^{st} as $u_{x1}^{st}/u_{x2}^{st} = -K_{t1}/K_{t2}$. By using this the stick displacements can be derived as follows

$$u_{x1}^{st} = \frac{u_{tot}}{1 + K_{t2}/K_{t1}} \quad \text{and} \quad u_{x2}^{st} = -\frac{u_{tot}}{1 + K_{t1}/K_{t2}} \tag{18}$$

By using (18) the friction force during stick can be derived from (15). The normal force and friction force are introduced in the resonator equation (3) by calculating the generalised forces

$$\mathbf{Q_N} = F_N \hat{\mathbf{e}}_n \frac{\partial \mathbf{L}}{\partial \mathbf{r}} \quad \text{and} \quad \mathbf{Q}_\mu = -\text{sign}\left(u_{x1}^{st}\right) F_\mu \hat{\mathbf{e}}_t \frac{\partial \mathbf{L}}{\partial \mathbf{r}}$$

where $\hat{\mathbf{e}}_n$ and $\hat{\mathbf{e}}_t$ are normal and tangential unit vectors, $\mathbf{L}$ is the coordinate of the contact tip and $\mathbf{r}$ is the vector of generalised coordinates from (3). The equations to be solved for the contact are

$$\mathbf{M}\ddot{\mathbf{r}} + \mathbf{C}\dot{\mathbf{r}} + \mathbf{K}\mathbf{r} = \mathbf{Q}_N + \mathbf{Q}_\mu \tag{19}$$

$$J\dot{\Omega} + C_R\Omega = \text{sign}(v_1 - v_2)RF_\mu - \tau_{app} \quad \text{during slip}$$

$$J\dot{\Omega} + C_R\Omega = \text{sign}(u_{x1})RF_\mu - \tau_{app} \quad \text{during stick}$$

where R is the rotor radius. It can be shown that the generalised forces in (19) are equivalent to those in (3), [1]. The condition for a transition from contact to no contact and vice versa is determined from the sign change of δ. The condition for a transition to stick is a change of sign of $(v_1 - v_2)$. Each stick calculation of F_μ is tested to see if $F_\mu < F_N$. If $F_\mu > F_N$ then a transition to slip is taken.

Simulation results

In order to demonstrate the contact model figure 5 presents different simulations. The resonance frequencies for 1st and 2nd bending mode are $f_{1n} = 13.5$ kHz and $f_{2n} = 51.7$ kHz. Figure 5a shows the unconstrained and constrained trajectories for an excitation of the type in eq. (1) with indications

for slip, stick and impact. Figure 5b shows the corresponding curves for the horizontal position of the

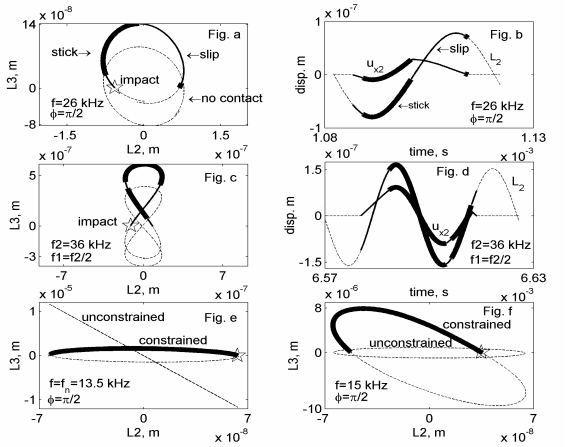

***Fig 5**: Simulation results.*

tip (L_2) and the tangential contact spring displacement (u_{x2}). Figure 5c-d shows similar simulations for an excitation of the type in eq. (2). Due to the small vibration amplitude the motion is almost not affected by the contact. This is not the case in figure 5e where the resonator is excited in the first resonance frequency (eq. (1)) in order to generate large vertical vibration amplitude. The vertical amplitude is clearly damped due the contact. Figure 5f shows the effect of contact resonance since the constrained vertical amplitude is greater the unconstrained vertical amplitude. Due to the small horizontal vibration amplitude stick is dominating in the cases shown.

Experimental results

It was not possible to compare simulation results with experiments and, furthermore the experiments were rather difficult to reproduce. However, it was still possible to obtain some interesting characteristics as shown in figure 6. Figure 6a and 6c show measurements of rotor velocity and load torque at two frequencies where peaks of the tangential vibration amplitude were observed. The characteristics at 44.5 kHz exhibit high torque but low velocity whereas the characteristics at 46kHz have opposite behaviour. The excitation voltage is of the type in eq. (1) with $\phi = \pi$. In order to explain the differences it was attempted to measure the tip trajectories at the two frequencies. However, as can be seen in figure 6b and 6d the frequencies of amplitude peaks have shifted and, thus, it was not possible to make any clear conclusion. However, the trajectories give some information about the vibration amplitudes required to obtain piezomotor performance. In comparison the horizontal vibration amplitudes shown in figure 5 are too small. The vertical amplitude of the ellipses is not caused by a 1st vibration mode but is caused by excitation of some other unknown vibration mode.

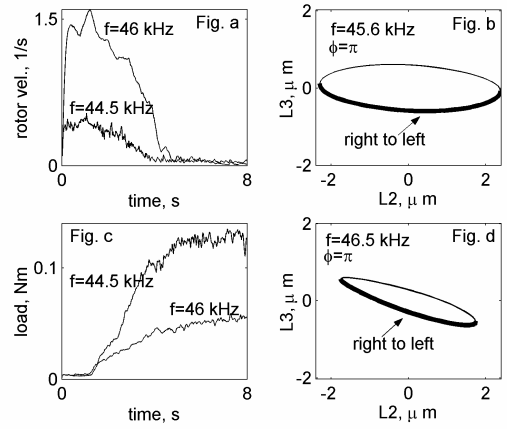

***Fig 6**: Experimental results.*

Conclusion

A new contact model with slip/stick has been developed for a standing wave piezomotor. Simulations of a bending resonator with inclusion of the contact model show well-behaved solutions of the numerical contact calculations. The simulations show that the tip trajectories in general cannot be prescribed. Experimental investigations of a piezomotor based on a bending resonator were conducted. The experimental results show the resonator principle does not work as intended since the vibration amplitudes are too small. However, motor performance was still achieved but it was due to excitation of an unknown mode.

References

[1] B. Andersen, M. Blanke, J. Helbo, Two-mode resonator and contact model for standing wave piezomotors, in proceedings of ASME 2001 design engineering technical conferences. 2001.

[2] N.W. Hagood, W.H. Chung, A. von Flotow, Modelling of Piezoelectric Actuator Dynamics for Active Structural Control, J. of Intell. Mat. Syst. and Struct., vol. 1 (1990), 327-355.

[3] K. L. Johnson, Contact Mechanics, Cambridge University Press, 1985.

[4] T. Maeno, D.B. Bogy, Effect of the Rotor/Stator Interface Condition Including Contact Type, Geometry, and Material Performance of Ultrasonic Motor, J. of Tribology, vol. 116 (1994), 726-732.

[5] N. Maw, J. R. Barber, J. N. Fawcett, The Oblique Impact of Elastic Spheres, Wear, vol. 38 (1976), 101-114.

[6] P. Vasiljev, R. Bareikis, The Travelling Wave Ultrasonic Motor With Quarterwave Electrodes, J. of Vibroengineering, vol. 5 (2000), 127-130.

[7] O.Yu. Zharii, An exact solution of a time dependent frictional contact problem for two

elastic spheres, Int. J. of Eng. Science, vol. 34 (1996), 537-548.